7th International Symposium on High-Temperature Metallurgical Processing
Edited by: Jiann-Yang Hwang, Tao Jiang, P. Chris Pistorius, Gerardo R.F. Alvear F., Onuralp Yücel, Liyuan Cai, Baojun Zhao, Dean Gregurek, and Varadarajan Seshadri
TMS (The Minerals, Metals & Materials Society), 2016

ORIGIN AND EVOLUTION OF NON-METALLIC INCLUSIONS FOR Al-KILLED STEEL DURING EAF-LF-VD-CC PROCESS

TANG Hai-yan[1,2], GUO Xiao-chen[2] , CHENG Peng-fei[2], LIANG Yong-cang[2], LI Jing-she[2], ZHAO Baojun[3]

[1]State Key Laboratory of Advanced Metallurgy, University of Science and Technology Beijing; No.30 Xueyuan Road; Beijing, 100083, China
[2]School of Metallurgical and Ecological Engineering, University of Science and Technology Beijing; No.30 Xueyuan Road; Beijing, 100083, China
[3]School of Chemical Engineering, The University of Queensland, Brisbane, Australia

Keywords: Al-killed steel; Inclusions; Origin; Evolution

Abstract

The origin and evolution of non-metallic inclusions for Al-killed casing steel during EAF-LF-VD-CC process were studied by industrial tracer experiments. The formations of Al_2O_3 and $MgO{\cdot}Al_2O_3$ micro- and macro-inclusions from ladle slag were analyzed by theoretical calculations. The results show that micro-inclusions were formed during deoxidation and temperature decreasing in the process of casting, most of the macro-inclusions come from entrapped ladle and mold slags. In addition, most of the Al_2O_3 formed were modified into $12CaO{\cdot}7Al_2O_3$ and $3CaO{\cdot}Al_2O_3$ inclusions which are liquid at steelmaking temperature. MnS cannot be fully modified to CaS and it was only wrapped outside the alumina or calcium aluminate in the form of (Ca,Mn)S with the amount of Ca-Si wire fed during the test.

Introduction

Casing is one of the important materials for oil fields which can reinforce the wall of an oil well and protect the hole, and its destruction can lead to the failure of a complete well. Therefore, not only are high strength, uniform and stable qualities, and strong corrosion and wear resistances required for casings, but also high capacity to support all kinds of loads such as pulling, pressing, twisting, and bending is needed [1]. Many factors can influence the performance of casing steel. A trail in a steel factory in China showed that the non-metallic inclusions were one of the main causes. However, the origin of the inclusions is very complicated which may come from deoxidation, ladle/tundish/mold slags or furnace lining. In order to control effectively the non-metallic inclusions in production, it is necessary to understand their origin and formation mechanisms. In this paper, the origin and evolution of non-metallic inclusions for Al-killed casing steel during EAF-LF-VD-CC process were studied by industrial tracer test. The formation mechanisms were discussed base on the industrial test.

Industrial trials and study methods

The industrial trials were performed for the production of three heats casing steel with the element compositions in billets (mass/%) C: 0.39~0.40, Si: 0.21~0.23, Mn: 1.52~1.56, P:

0.014~0.015, S: 0.006~0.008, Als: 0.02~0.03, V: 0.12, T.Ca: 0.0012~0.0016, Mg: 0.0003. The production route was 150t EBT—EAF→LF→VD→Ca-Si treatment→CC.

During electric arc furnace (EAF) tapping, a certain amounts of Si-Fe, Mn-Fe alloys and Al particles were added into the molten steel in the ladle for preliminary deoxidation combined with argon stirring. Synthesis slag was also added to desulphurize and decrease the contents of FeO and MnO. When the ladle reached the refining station (LF), Al wires were fed to further deoxidize and then the graphite electrodes were switched to heat the molten steel and adjust the slag composition. After LF treatment, the ladle reached vacuum degas (VD) station to remove gases such as O_2, N_2 and H_2. Then Ca-Si wires were fed to modify the high melting point inclusions. A 30t tundish and six-strand curved type continuous caster were equipped. The cross section of the round billet is Φ350mm.

In order to define the origin of the inclusions, tracers were used in this trial. BaCO3, which was equivalent to 8 mass% ladle slag, was mixed into the ladle slag to trace if the ladle slag was entrapped into the molten steel. 7 mass% of CeO_2 was mixed into the tundish slag, and 7 mass% La_2O_3 was added into tundish paint when constructing a new tundish. They were used to trace the entrapment of tundish slag and paint. Na_2O and K_2O were used to determine the entrapment of mold slag.

Steel and slag samples were taken before and after LF refining, after Ca treatment, in tundish and billets. The compositions of the steel samples were analyzed by ICP-AES (Inductively Coupled Plasma-Atomic Emission Spectrometry) and Carbon/Sulphur analyzer. The total oxygen (T.O.) and nitrogen were analyzed by TC−436 oxygen/nitrogen analyzer from Leco, USA. The slag was analyzed by chemical method. Micro-inclusions on the cross section f each steel sample were detected and analyzed by SEM-EDS to obtain their morphologies, sizes and chemical compositions. Macro-inclusions larger than 50μm were obtained by electrolysis method with non-water solution.

Results

Total oxygen and nitrogen in steel samples

Total oxygen contents in the steels include dissolved and compounded oxygens and it can well reflect the cleanliness of the steel. The change in nitrogen content is an indicator of the air absorbed during transportation of molten steel [2,3]. The averages of total oxygen and nitrogen contents of steel samples in different steps are shown in Figure 1. It can be seen that the total oxygen was decreased from 62ppm to 37ppm during LF refining, and it was 21ppm after VD calcium treatment, showing that the LF and VD were effective for oxygen removal. The total oxygen was increased by 2ppm in the tundish, indicating reoxidation could occur during casting which was confirmed by the increase of nitrogen content from 67ppm to 80ppm during the process. This suggests that the protection measure for the long nozzle needs to be improved. The total oxygen of head billet was 29ppm, which was significantly higher than other billets such as

normal, continuous casting and tail billets. This could be caused by instable casting which resulted in slag entrapment and reoxidation.

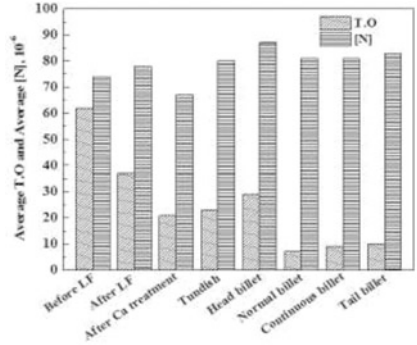

Figure1.Variation of the average T[O] and [N] in steel samples

Evolution of non-metallic inclusions in different stages

Before LF refining, the observed inclusions are mainly pure Al_2O_3 (Figure 2(a)), Al_2O_3–based inclusion (Figure 2(b)) and MnS inclusion (Figure2(c)). Al_2O_3 was formed by the reaction of Al and [O] in molten steel, Al_2O_3–based inclusion was formed by the compounded deoxidation of Al, Si and Mn, and MnS was precipitated by the solidification of molten steel due to high Mn content (1.54 mass%). Some of MnS show string shape, distributing around intergranular, which will cause anisotropy of steel.

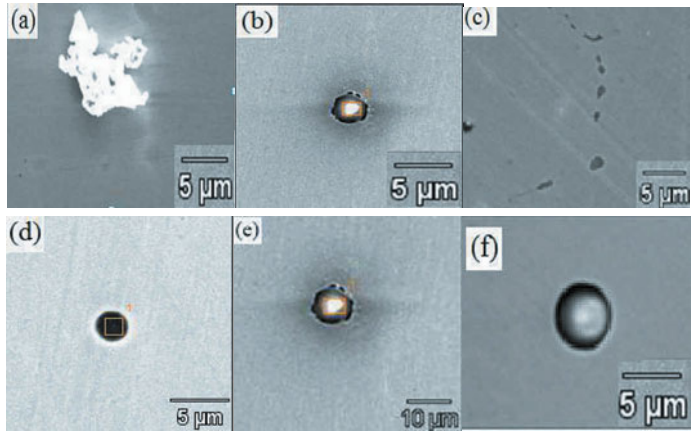

Figure 2 The typical microinclusions observed, (a) Al_2O_3, (b) Al_2O_3–based inclusion, (c) MnS, (d) MgO-Al_2O_3, (e) CaO-Al_2O_3-SiO_2-MgO, (f) 12CaO·7Al_2O_3

After LF, the inclusions were mainly transferred into $MgO\text{-}Al_2O_3$ (Figure 2(d)) and $CaO\text{-}Al_2O_3\text{-}SiO_2\text{-}(MgO)$ (Figure 2(e)) due to steel-slag and steel-refractory interface reactions, mostly less than 5 m in size. After VD degas, Ca-Si wire was fed into the molten steel, most of the inclusions were modified into spherical calcium aluminate $12CaO\cdot 7Al_2O_3$ (Figure3(f)) and $CaO\text{-}MgO\text{-}Al_2O_3$ type inclusions**.** Some of these inclusions were wrapped with (Ca,Mn)S with the size 2～20 m. The amount of MnS was significantly decreased during LF and VD refining and they were mostly coexisted with oxides in the form of (Ca,Mn)S, and hardly pure CaS was found.

Macro-inclusions in steel samples

Macro-inclusions refer to those larger than 50μm and they were extracted with electrolysis method. Figure 3 shows the typical morphologies of some macro-inclusions and their EDX patterns.

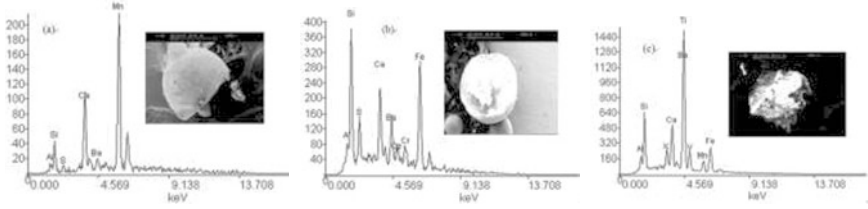

Figure 3 Morphology and energy spectrum of typical macroinclusions (a) after LF samples; (b) billet samples; (c) billet samples

It can be seen from Figure 3(a) that the macro-inclusion in the steel after LF contains Ba, indicating this type of macro-inclusions originated from ladle slag. Figures 3(b) and 3(c) show macro-inclusions in billets contain Ba, Ce and K, indicating ladle slag, tundish refractory and mold slag were entrapped into the molten steel to form complicated macroinclusions. The details will be discussed in the following sections.

Discussions

Effect of [Ca] and [Al] contents in molten steel on the compositions of the precipitated inclusions during LF refining

In order to control the inclusions in practice, the thermodynamic analysis for the formation of the inclusions during LF refining is performed. The activity coefficient of each element and activity in liquid steel is calculated by Eqs. (1) and (2).

$$\lg f_i = \sum_j e_i^j [\text{mass}\%j] \qquad (1)$$

$$a_{[i]} = f_i \cdot [\text{mass}\%i] \qquad (2)$$

Where e_i^j represents the first order interaction coefficient of elements j to i relative to diluted solution, and $a_{[i]}$ is the activity of component i relative to mass 1% diluted solution. Table 1 lists

the calculated activity coefficient of each element in liquid steel at 1873K. In the calculation, the composition of the liquid steel is (mass%): C, 0.39; Si, 0.22; Mn, 0.52; S, 0.007; P, 0.015; Al, 0.02; Ca_T, 0.0016. The interaction coefficients of the elements in liquid steel are taken from the references [4,5].

Table 1 Activity coefficients of elements in liquid steel at 1873 K for casing steel [4,5]

T	f_C	f_{Si}	f_{Mn}	f_{Al}	fS	f_O	f_{Mg}
1873K	1.139	1.259	0.938	1.062	0.953	0.492	0.767

Table 2 Deoxidation reactions in liquid steel and related equilibrium constant expressions [6]

Reaction equation	ΔG^0/(J/mol)	Eq.
$[Si]+2[O]=SiO_2(s)$	$\Delta G^0 = -581900+221.8T$ J/mol	(3)
$2[Al]+3[O]=Al_2O_3(s)$	$\Delta G^0 = -1202000+386.3T$ J/mol	(4)
$6[Al]+2[Si]+13[O]=3Al_2O_3(s)\cdot 2SiO_2$	$\Delta G^0 = -47741543+1592T$ J/mol	(5)
$[Ca]+[Si]+3[O]=CaO\cdot SiO_2$	$\Delta G^0 = -1301477+359.73T$ J/mol	(6)
$[Ca]+2[Si]+2[Al]+8[O]=CaO\cdot Al_2O_3\cdot 2SiO_2$	$\Delta G^0 = -3088133+942.88T$ J/mol	(7)
$2[Ca]+2[Al]+[Si]+7[O]=2CaO\cdot Al_2O_3\cdot SiO_2$	$\Delta G^0 = -3190946+861.23T$ J/mol	(8)

In order to improve the casing quality, the main task of LF refining is to decrease the amount of inclusions and control their compositions in the fully-liquid zone at the refining temperature. During LF refining, due to the steel-slag interaction, different types of inclusions may be formed. According to the ternary phase diagram $CaO\text{-}A1_2O_3\text{-}SiO_2$ [7], the possible precipitated non-metallic inclusions include Al_2O_3, SiO_2, CA_X, $3Al_2O_3\cdot 2SiO_2$ (short for A_3S_2), $CaO\cdot Al_2O_3\cdot 2SiO_2$ (CAS_2), $2CaO\cdot Al_2O_3\cdot SiO_2$ (C_2AS), $CaO\cdot SiO_2$ (CS), in which the eutectic area of CAS_2 and CS is expected with lower melting temperature. These substances could be formed by the deoxidation reactions [6].

The activities of precipitated phases in Eqs (3)~(8) are taken as unity, substituting the activities coefficient in Table 1, the stable phase zone of the above mentioned substances can be obtained as shown in Figure 4. It can be seen that Al_2O_3 inclusion is easily formed when the acidic dissolved aluminum, $[Al]_s$, is over 3ppm. To control the compositions of the inclusions in eutectic area of CS and CAS_2, the required $[Al]_s$ is between 0.1~20ppm and $a_{[Ca]} < 9.2\times10^{-10}$. The acidic dissolved aluminum is about 0.01~0.03% during LF refining, CS and CAS_2 are not able to form and only Al_2O_3 inclusion is stable. Figure 5 shows the relationship of $[Al]_s$ and $a_{[Ca]}$ when forming CAS_2 and C_2AS. Compared with Figure 4, the concentration range to form C_2AS is in the same range to form CS and Al_2O_3, thus CS and Al_2O_3 will be formed prior to C_2AS. This means C_2AS inclusion cannot be formed in the present LF process conditions. As a result, the main inclusion during LF refining is Al_2O_3, which is consistent with the observations in the experiments.

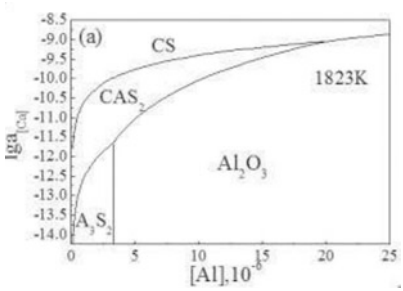

Figure 4 Effect of [Ca] and [Al] contents on deoxidation products at 1873K

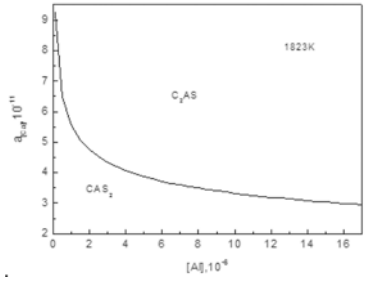

Figure 5 $a_{[Ca]}$-[Al] relationship when forming CAS_2 and C_2AS

Formation of $MgO{\cdot}Al_2O_3$: It is observed from the experiments that, $MgO{\cdot}Al_2O_3$ spinel type inclusions exist in the steel samples after LF and Ca treatment. There are three types of spinel observed. One is the isolated spherical spinel, mainly containing Mg, Al, and O elements in small quantities. The second type is the modified spinel type inclusion containing Mg, Al, Ca, O and a little Si**,** it is the main existence form. The third type is the MgO Al_2O_3 spinel as core wrapped with sulphides.

Comparing the steel samples taken at different steps, it was found that there was very little $MgO{\cdot}Al_2O_3$ spinel type inclusions observed before LF refining, but they began to occur after LF. This can be explained by the following equations. The acidic dissolved [Al] in molten steel reacts with MgO in slag and lining to generate [Mg], then reacting with Al_2O_3 to form MgO Al_2O_3 [8].

$$4(MgO)+2[Al]=(MgO\cdot Al_2O_3)+3[Mg] \tag{9}$$

$$\log K_1=-33.09+50880/T=\log\frac{f_{\%,Mg}^3[\%Mg]^3\cdot a_{MgO\cdot Al_2O_3}}{f_{\%,Al}^2[\%Al]^2\cdot a_{MgO}^4} \tag{10}$$

$$4(Al_2O_3)+3[Mg]=3(MgO\cdot Al_2O_3)+2[Al] \tag{11}$$

$$\log K_1=-34.37+\frac{46950}{T}=\log\frac{f_{\%,Al}^2[\%Al]^2\cdot a_{MgO\cdot Al_2O_3}^3}{f_{\%,Mg}^3[\%Mg]^3\cdot a_{Al_2O_3}^4} \tag{12}$$

The phase stability diagram of MgO / MgO Al_2O_3 / Al_2O_3 can be calculated by the Eqs. (9) ~ (12). According to Fujii et al. [9], the activity of $MgO{\cdot}Al_2O_3$ is taken as 0.8 and that of MgO as 0.99 for Eq. (2) at 1873 K due to the very small solubility of Al_2O_3 into MgO. Meantime, the activity of $MgO{\cdot}Al_2O_3$ and Al_2O_3 are taken as 0.47 and 1 respectively for Eq. (2) since there is no solubility of MgO into Al_2O_3[9]. The phase stability diagram is shown in Figure 6. It can be seen that contents of dissolved [Al] and [Mg] in molten casing steel are mainly in the formation region of $MgO{\cdot}Al_2O_3$ as signed in the Figure. The results are consistent with the experiments. The quantity of $MgO{\cdot}Al_2O_3$ spinel type inclusion was increased after VD treatment and occurred mostly in the composite oxide form. This is the modified product of MgO Al_2O_3 spinel inclusion due to Ca-Si wire feeding after VD treatment. The researches of Itoh et al.[10] and YANG et al.[11]

showed that about 1 ppm Ca in the steel could significantly decrease the stability of MgO Al_2O_3 spinel inclusions and made them modifying into MgO-Al_2O_3-CaO inclusions. The dissolved calcium is about 1.2 ~ 3.0ppm after Ca-Si wire feeding, so more MgO-Al_2O_3-CaO type inclusions were observed.

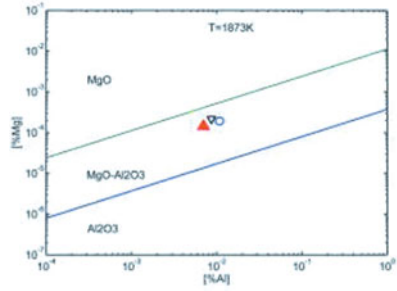

Figure 6 Phase stability diagram of MgO/MgO·Al_2O_3/Al_2O_3

Macro-inclusions from the ladle

Many observed macro-inclusions contain tracer Ba, indicating ladle slag is entrapped into the molten steel. When the argon flowrate is higher, slag entrapment will occur on the steel-slag interface. The critical Weber Number is 6.796 according to the reference [12]:

$$w_e = F_S / \sqrt{F_g F_\sigma} = \rho_s u_p^2 / [g\sigma_{s-m}(\rho_m - \rho_s)]^{1/2} = 6.796 \qquad (13)$$

$$u_p = \sqrt{6.796 \frac{[g\sigma_{s-m}(\rho_m - \rho_s)]^{1/2}}{\rho_s}} \qquad (14)$$

Where u_p is the horizontal velocity of liquid steel at slag entrapment, σ_{s-m} is steel-slag interfacial tension, ρ_m and ρ_S are densities of steel and slag respectively.

Substituting σ_{s-m} = 1.2 N/m, ρ_m = 6890 kg/m^3, ρ_S = 3000 kg/m^3 [2,12], u_p is calculated to be 0.7.

$$u_p = 4.177 \times (1-\alpha)^{1/12} \frac{Q^{1/3} H^{1/4}}{R^{1/3}} = 0.7$$

Assuming α = 8%, the critical argon flowrate Q of slag entrapment for 150t ladle is 183.3 L/min. In industrial production, the flowrate blown during LF is 510.9~608.5 L/min, much higher than that calculated, thus slag entrapment is inevitable.

Conclusions

(1) Before LF refining, the observed microinclusions are mainly pure Al_2O_3, Al_2O_3–based and MnS inclusions. Al_2O_3 is formed by the reaction of Al and [O] in molten steel, Al_2O_3–based inclusion is formed by the compounded deoxidation of Al, Si and Mn, and MnS is precipitated by the solidification of molten steel.
(2) Most Al_2O_3 inclusions are modified into $12CaO{\cdot}7Al_2O_3$ 和 $3CaO{\cdot}Al_2O_3$ inclusions which are liquid at steelmaking temperature, while MnS cannot be fully modified into pure CaS and it can only be wrapped outside the alumina or calcium aluminate in the form of (Ca,Mn)S with the amount of Ca-Si wire fed in the trials.
(3) Macroinclusions originated from the ladle slag, tundish cover and mold slag. The gas flowrate during LF refining is much higher than that required for slag entrapment.

Acknowledgements

The authors are grateful for the support from the State Key Laboratory of Advanced Metallurgy of the USTB (No. 41603014) and the National Natural Science Foundation of China (No. 51374021).

References

[1] X.M. Dong, Q.C. Tian, Q.A. Zhang, "Corrosion behaviour of oil well casing steel in H_2S saturated NACE solution", *Corros. Eng. Sci. Techn.,* 45(2010) 181-185.
[2] H.Y. TANG, J.S. LI, "Thermodynamic analysis on the formation mechanism of magnesium-aluminum MgO Al_2O_3 spinel type inclusions in casing steel", *International Journal of Minerals, Metallurgy and Materials,* 17(1) (2010), 32-38.
[3] H.Y. TANG, J.S. LI, "Effect of flow control devices of tundish on cleanliness of billets", *Journal of Iron and Steel Research International*, 15, (2008), 499-504.
[4] G. K. Sigworth and J.F. Elliot, "The thermodynamics of liquid dilute iron alloys", *Metal Science*, 18(1974), 298-310.
[5] S.W. Cho and H. Suito, "Assessment of calcium-oxygen equilibrium in liquid iron", *ISIJ Int.*, 34 (3) (1994), 265-269.
[6] Z.L. Xue, "Control on oxide inclusions composition and shape in spring steel", (PH.D. thesis, Iron and Steel Research Institute, 2001), 22.
[7] Verein Deutscher Eisenhüttenleute, Slag Atlas 2th Edition, Verlag Stahleisen GmbH, 1995.
[8] Z.Y. Deng, M.Y. Zhu., "Evolution Mechanism of Non-metallic Inclusions in Al-Killed Alloyed Steel during Secondary Refining Process", *ISIJ international,* 53(3) (2013), 450-458.
[9] K. Fujii, T. Nagasaka and M. Hino. Activities of the Constituents in Spinel Solid Solution and Free Energies of Formation of MgO, $MgO{\cdot}Al_2O_3$. *ISIJ Int.,* 40 (2000), 1059-1066.
[10] W. Yang, L.F. Zhang, X.H. Wang, et al., Characteristics of Inclusions in Low Carbon Al-Killed Steel during Ladle Furnace Refining and Calcium Treatment, *ISIJ Int.,*53 (8) (2013) 1401-1410.
[11] H. Itoh, M. Hino, B.Y. Shiro, Thermodynamics on the Formation of Spinel Nonmetallic Inclusion in Liquid Steel, *Metall. Mater. Trans. B* 28 (1997), 953-956.
[12] Z.Q. Xiao, L.X. Hu, "Research on the behavior of large particles and their sources of inclusions blowing steel", *Iron & Steel*, 23(1) (1988), 23~26.